Polym. Bull. (2011) 66:747–760
DOI 10.1007/s00289-010-0307-9

ORIGINAL PAPER

Electrochemical polymerization of 2-aminothiazole

Hakan Çiftçi · Hasan Nur Testereci · Zeki Öktem

Received: 19 December 2009 / Revised: 28 April 2010 / Accepted: 23 May 2010 /
Published online: 4 June 2010
© Springer-Verlag 2010

Abstract Electrochemical polymerization of 2-aminothiazole (AT) was studied in acetonitrile with tetrabutylammonium tetrafluoroborate (TBAFB) as the supporting electrolyte via constant potential electrolysis (CPE). The redox behavior of AT was investigated in the same solvent-electrolyte couple by cyclic voltammetry, CV. CPE of AT produced a soluble conducting polymer on the electrode surface. The effects of temperature, monomer concentration and polymerization time on the rate of electrochemical polymerization were also studied. The structural analyses of the polymer were carried out by ^{1}H-NMR, FTIR and UV–VIS spectroscopies and elemental analysis. Thermal properties were studied by DSC and TGA. Conductivity measurements were carried out by four-probe technique and the number average molecular weight, M_n, of the polymer was determined by cryoscopy.

Keywords Conducting polymer · Cyclic voltammetry · Electrochemical polymerization · Poly(2-aminothiazole)

Introduction

There are many studies in the literature concerning the synthesis of conducting polymers because of their applications as biosensors [1, 2], corrosion inhibitors [3, 4], ion sensors [5, 6], and uses in electrochromic display devices [7, 8], and electrochemical batteries [9, 10]. Therefore, conducting polymers such as polyaniline [4, 10, 11], polypyrrole [12, 13], polythiophene [14, 15], and several polyaromatic amines [16, 17] were synthesized and characterized.

H. Çiftçi · H. N. Testereci · Z. Öktem (✉)
Department of Chemistry, Faculty of Arts and Sciences, Kırıkkale University,
71450 Yahşihan, Kırıkkale, Turkey
e-mail: zoktem@kku.edu.tr

Several studies on the chemical and electrochemical polymerization of thiazole and some thiazole derivatives have been carried out [18–23]. The conductivities of these polymers were reported to be in the range of 10^{-4}–10^{-8} S/cm. Bolognesi et al. [19] reported that the conductivity of 2,5-polythiazole increased from 10^{-12} S/cm up to 10^{-7}–10^{-8} S/cm upon doping with AsF_5 and Na-benzophenone. On the other hand, conductivity values of Na-doped poly(thiazole-2,5-diyl), poly(4-methylthiazole-2,5-diyl) and poly(4,4′-dimethyl-2,2-thiazole-5,5′-diyl) were reported to be in the order of 10^{-4} S/cm [20]. Polymerization mechanisms including the oxidation and reaction of $-NH_2$ group were suggested for the electrochemical polymerization of AT[21] and AT derivatives [22, 23]. Solmaz et al. [21], reported that the electrochemical polymerization of AT by CV technique in 0.3 M aqueous ammonium oxalate solution, by potential cycling between −0.20–1.40 V, produced a small amount of insoluble conducting film (1.88×10^{-6} S/cm) on the Pt electrode surface.

In this work, we report the electrochemical synthesis of soluble and conducting poly(2-aminothiazole) (PAT) with high conversions. The effects of polymerization time, temperature, and concentration of monomer on the rate of electrochemical polymerization were also presented. Furthermore, results of elemental and spectroscopic analyses were discussed together with the mechanism of the electrochemical polymerization.

Experimental

Materials

The monomer AT (2-aminothiazole; Aldrich Chemical Co., 90%) was purified by recrystallization from methanol. Acetonitrile was purified by drying over CaH_2 followed by fractional distillation. Tetrabutylammonium tetrafluoroborate (TBAFB; Aldrich Chemical Co.) was used without further purification as supporting electrolyte for constant potential electrolysis (CPE) and CV measurements. All other chemicals were of analytical reagent grade and used as received.

Cyclic voltammetry

The redox behavior of the monomer and polymer was determined by CV. The system consisted of a potentiostat (Gamry Instruments, Reference 600, Potentiostat/Galvanostat/ZRA) and a CV cell containing a Pt-wire working electrode, a Pt-wire counter electrode and a $Ag°/Ag^+$ as reference electrode. Measurements were carried out under N_2 atmosphere in acetonitrile at room temperature.

Polymer synthesis

Electrochemical polymerization of AT was achieved by CPE. The supporting electrolyte was dissolved in acetonitrile and then introduced together with the monomer solution into a H-type cell with two separated compartments. The working and counter electrodes were Pt foils with an area of 2.0 cm^2, and the reference

electrode was $Ag°/Ag^+$. Prior to CPE, the cell was placed in a constant temperature bath. Electrolyses were carried out under N_2 atmosphere at constant temperature. CPE of AT produced a dark brown polymer on the surface of Pt electrode. At the end of the electrolysis, polymer deposit was separated by scrubbing from the working electrode surface, washed with acetonitrile, and dried under vacuum at room temperature. The yield of electrochemical polymerization was calculated from the amount of obtained product.

Polymer characterization

^{1}H-NMR spectra of the polymers were taken by a Bruker Instrument-NMR Spectrometer (DPX-400) in DMSO-d_6. FTIR spectra of the samples were obtained on a Jasco, 480 Plus FTIR Spectrometer using KBr pellets. Elemental analysis was carried out using a LECO CHNS 932 elemental analyzer. A Perkin Elmer Diamond DSC, Pyris series instrument was used for DSC analyses. TGA thermogram of the polymer was recorded using a DuPont 950 thermogravimetric analyzer. UV–VIS absorption spectra of the samples were measured using a Hewlett Packard 8453A diode array UV–VIS Spectrometer in DMSO. A JSM 5600 model scanning electron microscope was utilized in analyzing the surface structure of the polymer. Four-probe technique was applied for the measurement of conductivities of the pressed disc samples at room temperature. Number average molecular weight, M_n, of the polymer was determined by cryoscopy. A well-closed system equipped with a Beckmann thermometer was used.

Results and discussion

Electrochemical behavior of AT

Electrochemical polymerization of AT was carried out in acetonitrile on Pt-electrodes. Prior to CPE, the oxidation–reduction behavior of AT was studied by CV in acetonitrile–TBAFB, solvent–electrolyte couple at room temperature. A voltammogram of AT is given in Fig. 1a. AT has an oxidation peak at about 2.70 V versus $Ag°/Ag^+$ reference electrode, representing an irreversible electron transfer. The multisweep cyclic voltammogram of AT showed that the peak at 2.70 V disappeared after the first cycle and a new peak at 2.20 V appeared (Fig. 1b).

However, the conversion obtained from the CPE carried out at 2.20 V was too low. The conversion was attempted to be increased by initiating the polymerization at 2.70 V for 10 min and then continuing at 2.20 V, but the results showed no positive change. Therefore, CPE of AT studied at 2.70 V, at which high conversions were obtained. On the other hand, the oxidation potential of the polymer was observed at 1.30 V (Fig. 2), thus the peak observed at around 2.20 V may be attributed to the oxidation of low molecular weight fractions such as dimer, trimer, etc.

Variation of peak current with the voltage scan rate was also studied. A negative slope was obtained when current function, $I/CV^{1/2}$, for the oxidation peak at 2.70 V was plotted against log V, where I is the peak current, V is the voltage scan rate, and

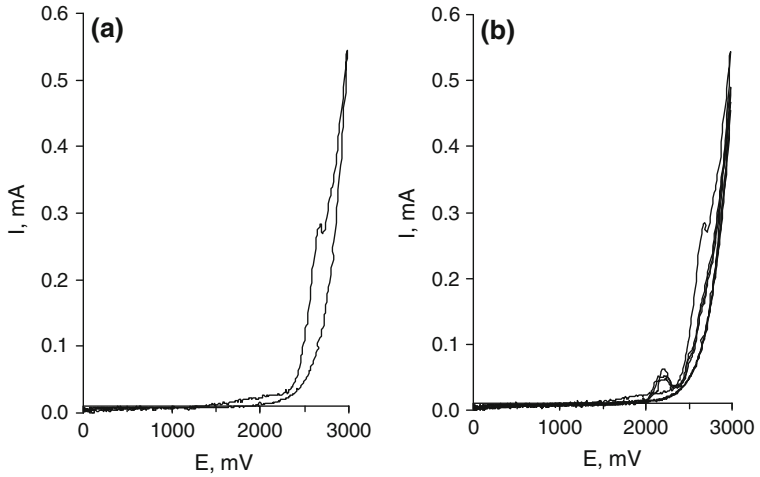

Fig. 1 CV (**a**) and multisweep CV (**b**) of 1×10^{-2} M AT measured in 0.1 M TBAFB–acetonitrile solution at room temperature. Voltage scan rate = 50 mV/s

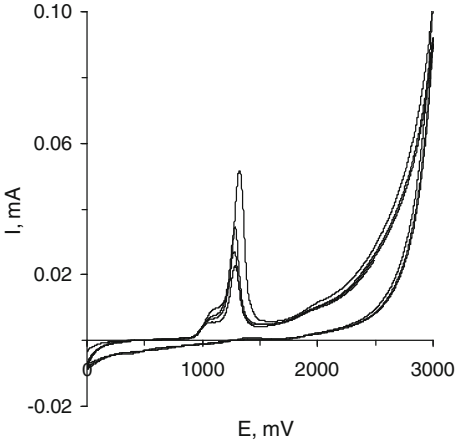

Fig. 2 Multisweep CV of PAT in 0.1 M TBAFB–acetonitrile solution at room temperature. Voltage scan rate = 50 mV/s

C is the concentration (Fig. 3a). The negative slope indicated a reversible one-electron transfer at 2.70 V versus $Ag°/Ag^{+}$, followed by a chemical reaction according to Nicholson–Shain criteria [24]. The absence of reversible peak in the voltammogram can be explained due to higher rate of chemical reaction following the electrochemical oxidation. Also, the linear plot of I versus $V^{1/2}$ indicated the occurrence of a diffusion controlled electron transfer reaction (Fig. 3b).

Electrochemical polymerization

Electrochemical polymerization was performed by anodic oxidation of a 0.2 M solution of AT in acetonitrile, in the presence of 0.1 M TBAFB at 2.70 V versus

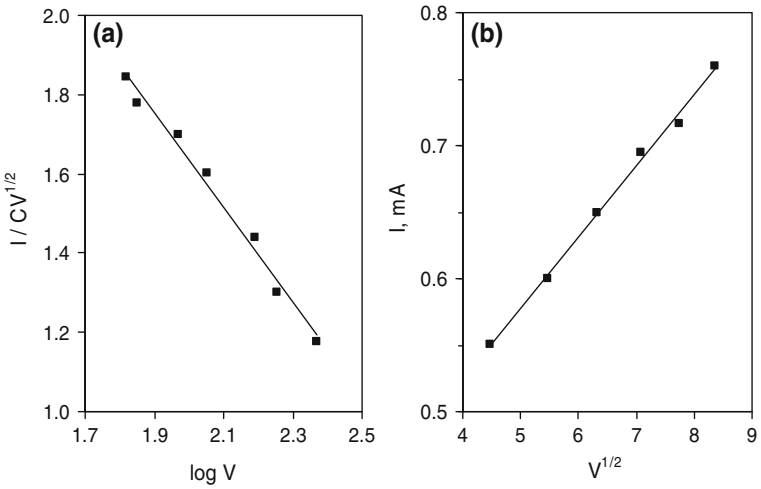

Fig. 3 Variation of current function ($I/CV^{1/2}$) with voltage scan rate (**a**) and peak current with the square root of voltage scan rate (**b**). *I* is current in mA, *C* is concentration in mol/L, and *V* is voltage scan rate in mV/s

$Ag°/Ag^{+}$. At the end of the electrolysis, a dark brown polymer was formed on the working electrode surface. The polymer was removed by scrubbing from the electrode surface, washed with acetonitrile, and dried under vacuum at room temperature.

The effect of temperature on the rate of electrochemical polymerization of AT was studied at 15, 25 and 40 °C. Plots of % yield versus electrolysis time for each temperature indicated that an increase in temperature resulted in an increase in the polymer yield (Fig. 4). Solmaz et al. [21] reported that the electrochemical polymerization of AT in aqueous ammonium oxalate solution produced only a small

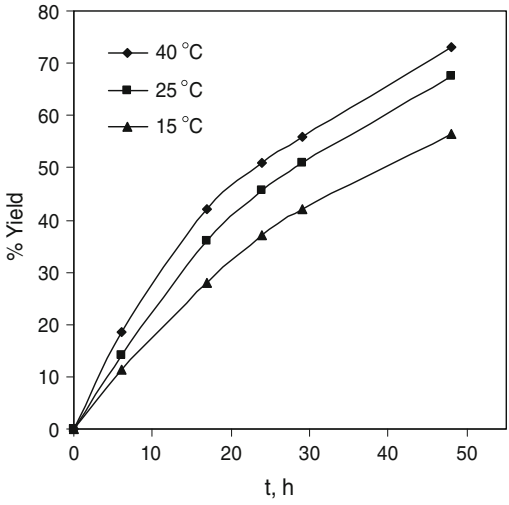

Fig. 4 Effect of temperature on the rate of electrochemical polymerization of AT at constant potential of +2.70 V. $C_{AT} = 0.2$ M, $C_{TBAFB} = 0.1$ M

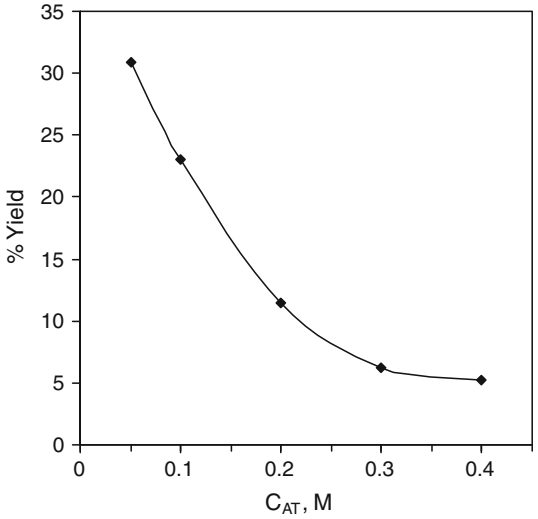

Fig. 5 Effect of AT concentration on the rate of electrochemical polymerization of AT at constant potential of +2.70 V. $C_{TBAFB} = 0.1$ M, $t = 6$ h, $T = 25$ °C

amount of insoluble polymer film on the Pt electrode. On the contrary, in acetonitrile-TBAFB solvent-electrolyte couple we obtained 65% yield at room temperature, which increased up to about 75% by increasing the temperature up to 40 °C (Fig. 4). Because of the obtained high yields, the rate of polymerization could be monitored gravimetrically.

The effect of monomer concentration on the rate of electrochemical polymerization of AT was also studied. The results obtained from the electrochemical polymerizations carried out at 25 °C for 6 h showed a decrease in polymer yield from about 30 to 5% upon increasing the monomer concentration from 0.05 to 0.3 M (Fig. 5). However, formation and increase in the amount of an unprecipitable oily product with the increase in the concentration of monomer was also observed. Therefore, the decrease in polymer yield probably was due to the increase in the formation of transfer reactions, which led to the formation of low molecular weight oily products.

Polymer characterization

The electrochemical polymerization of AT in acetonitrile-TBAFB produced a polymer on the working electrode by CPE at 2.70 V vs. $Ag°/Ag^{+}$. The yield of polymerization was high, about 65% at room temperature in 48 h (Fig. 4) and the polymer was found to be completely soluble in DMSO and DMF and partially soluble in dilute H_2SO_4(aq), NaOH(aq) and some other common organic solvents. Therefore, M_n of the polymer could be determined by cryoscopy technique with DMSO as the solvent [25]. The moisture absorption of DMSO was prevented by using a well-closed, specially designed, and constructed system. Cryoscopic constant, $K_f = M\Delta T/c$, was determined from the slope of the plot of $M\Delta T$ vs. c by using purified naphthalene as a standard, where M is the molecular weight of naphthalene, ΔT is the freezing point depression, and c is the solute concentration

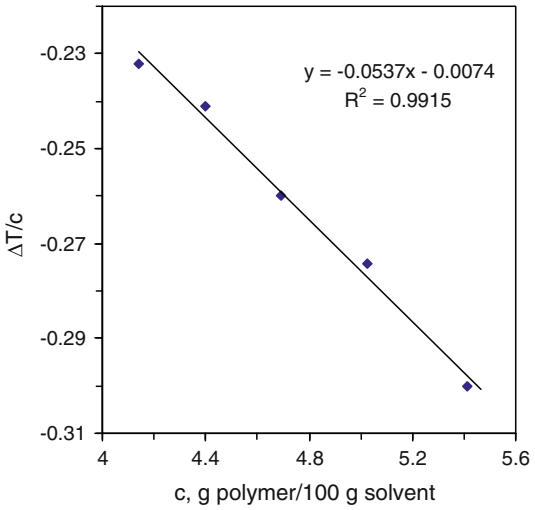

Fig. 6 Freezing point depression-concentration curve of PAT

per 100 g of the solvent. K_f is found to be equal to −54.18 °C·g/mol. M_n of the polymer, $M_n = K_f/(\Delta T/c)_{c=0}$, is calculated from the intercept of the ΔT vs. c plot as 7320 g/mol (Fig. 6).

The only source of sulfur in the polymerization medium was the monomer, AT. Assuming that there was no loss of S during the polymerization, then each S in the polymer chain should represent a polymerized AT ring. Therefore, by considering the results of elemental analysis (Table 1) and M_n of the polymer, the average degree of polymerization was calculated to be about 46. However, this value corresponds to a molecular weight, 4600 g/mol, which is much lower than the experimentally determined one (7320 g/mol). A comparison of the amount of the elements which obtained from the elemental analysis and calculated due to the empirical formula of AT, $C_3H_4N_2S$, where $n_C = 3n_S$, $n_H = 4n_S$ and $n_N = 2n_S$, showed that about 45 C, 87 H and 18 N present in excess in the polymer chain. Although the polymer washed with acetonitrile for several times, the excess amount of the elements may be attributed to the remained electrolyte among the polymer chains. Considering that each excess N should represent a $[CH_3(CH_2)_3]_4N^+$ group ($n_C = 16n_N$, $n_H = 36n_N$), then the excess amount of C and H in a chain should be 288 and 648, respectively. Therefore, the excess amount of the elements cannot be attributed mainly to the presence of electrolyte, hence n-Bu_4N^+ ions in the polymer.

The other probable source of N, C, and H in the polymerization medium was the solvent, acetonitrile. The reaction of acetonitrile during some CPE studies has been reported [26–29]. Calculations performed by assuming each excess N may represent

Table 1 Elemental analysis of poly(2-aminothiazole)

Elements	%C	%H	%N	%S
Found	30.04	3.74	21.02	20.13
Calculated	28.55	3.28	21.05	20.13

a reacted acetonitrile molecule in the polymer indicated an additional 36 C and 54 H would be introduced to the polymer by the reaction of acetonitrile. The results were close to the excess amount of the elements. Therefore, the percentages of the elements were calculated by assuming each S in the polymer represents a polymerized AT ring and each excess N is due to a reacted acetonitrile molecule. The calculated and experimentally obtained results were found to be in good agreement and are given in Table 1. In addition, elemental analysis indicated that about 25% of the polymer contains elements other than C, H, N, and S. Since PAT was found to be conducting (10^{-6} S/cm), this percentage may be attributed to the presence of BF_4^- ions [7, 16].

IR spectra of the monomer and that of polymers obtained from the CPE of AT are given in Fig. 7. The bands at 3410 and 3290 cm^{-1} in the spectrum of AT are associated with the asymmetrical and symmetrical N–H stretching modes of the $-NH_2$ group, respectively (Fig. 7a) [30]. The N–H stretching is observed at 3402 cm^{-1} as a single broad band in the spectrum of PAT (Fig. 7b). The probability of overlapping of this band with the stretching bands of remained electrolyte in the polymer was checked by using $NaClO_4$ instead of TBAFB, as the supporting electrolyte. The similar single broad band observed at 3112 cm^{-1} in the IR spectrum of the obtained polymer, PAT–$NaClO_4$, (Fig. 6c) indicated formation of –N(H)– linkages, hence the reaction of $–NH_2$ group during the CPE of AT.

The C=N stretching bands are observed at 1627, 1623 and 1654 cm^{-1} in the spectra of AT, PAT and PAT–$NaClO_4$, respectively. The bands at around 1520 cm^{-1} are due to C=C stretching vibration and the absorption bands between 1360–400 cm^{-1} and 1200–1230 cm^{-1} mainly arise from C–N and C–H vibrations, respectively. The bands at 643, 620, and 653 cm^{-1} in the spectra of AT, PAT and

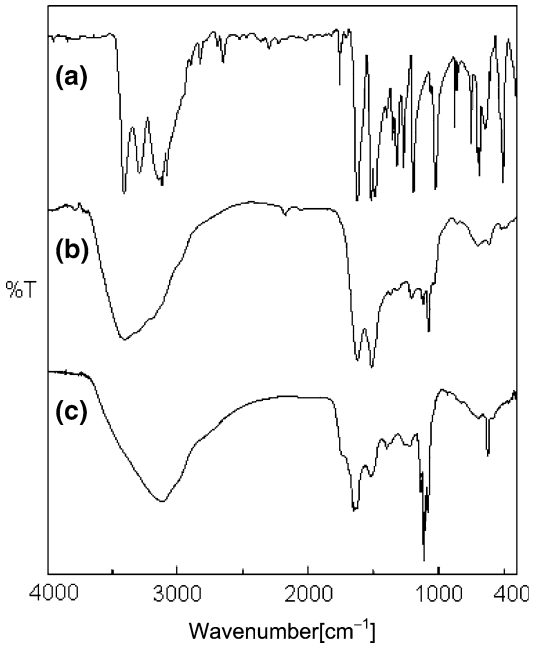

Fig. 7 FTIR spectra of AT (*a*), PAT (*b*) and PAT–$NaClO_4$ (*c*)

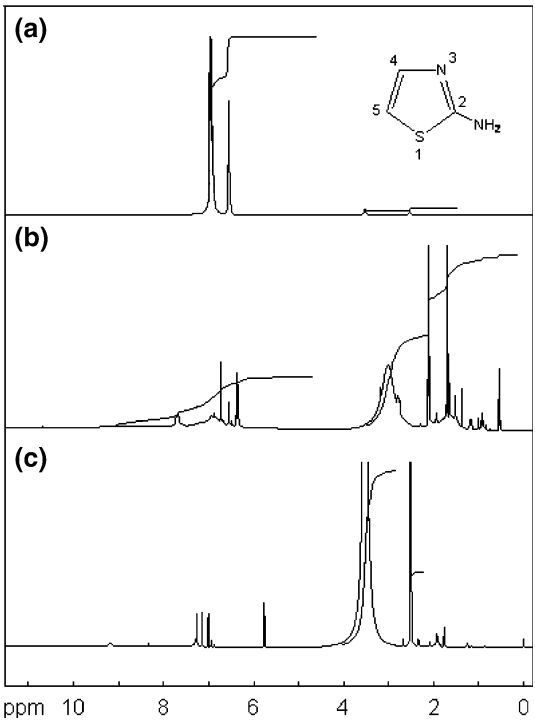

Fig. 8 ^{1}H-NMR spectra of AT (*a*), PAT (*b*) and PAT–$NaClO_4$ (*c*)

PAT–$NaClO_4$, respectively, are associated with the C–S stretching vibration. Also, the strong bands at around 1100 cm^{-1} in the spectra of the polymers are due to BF_4^- and ClO_4^- ions [7, 16, 27].

In Fig. 8, ^{1}H-NMR spectra of AT and the polymers obtained from the CPE of AT in acetonitrile are given. The signals at 6.53, 6.92 and 6.97 ppm in the spectrum of AT are assigned to the H5, H4 and $–NH_2$ protons, respectively (Fig. 8a) [30]. The strong signals at 2.5 and 3.5 ppm in the polymer spectra are due to DMSO and dissolved water, respectively. The assignments of various protons in the spectra of PAT (Fig. 8b) and PAT–$NaClO_4$ (Fig. 8c) are as follows: the signals at around 7.0 ppm are assigned to the =C(H)–N= and –C(H)=N– protons (H4 proton in different environment). The signals that can be assigned to $–NH_2$ groups bound to the aromatic ring and to an aliphatic group are observed at 6.87 and 1.75 ppm, respectively [30]. Also, the signals at 8.09 and 5.75 ppm in the spectra of PAT and PAT–$NaClO_4$ respectively, can be assigned to the N–H proton in the polymer chain. The weak signals between 1–4 ppm in the spectrum of PAT are assigned to the protons of acetonitrile, entered into the structure of the polymer.

Spectroscopic studies indicated a similar polymerization mechanism to the proposed mechanisms for the polymerization of AT and AT derivatives in different polymerization conditions through the formation of –N(H)– linkages [21–23]. In this mechanism, polymerization takes place by coupling of the radicals formed after the oxidation of $–NH_2$ and rearrangement of the molecule as,

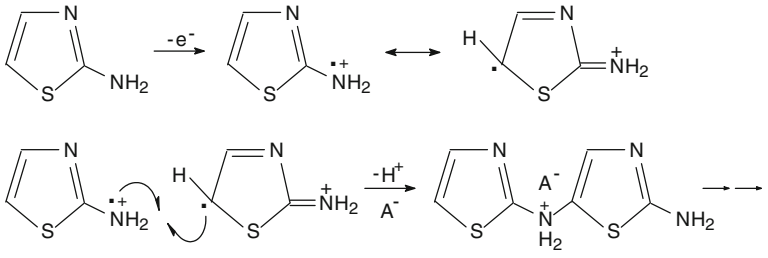

A^-: Electrolyte anion

Deprotonation of the formed structures and probably formation of HF during the polymerization of AT was also supported by the decrease in the initial pH of the polymerization medium from 8.4 to 5.4 upon CPE carried out at 25 °C for 6 h [26, 27, 31].

Results of elemental analysis indicated that a certain amount of acetonitrile entered into the structure of the polymer. Reaction of acetonitrile through a cationic mechanism in the electrochemical polymerization of styrene and 4-allyl-1,2-dimethoxybenzene was suggested previously [28, 29]. Spectroscopic studies did not indicate the presence of $-CH_3$ and $-C\equiv N$ groups in the structure of the polymer. Therefore, formation of structures such as $CH_3-\underset{|}{C}=N-R$ and $R-CH_2-C\equiv N$ were not expected. In the study of constant current electrolysis of styrene in sulpholane–$NaBF_4$ solvent–electrolyte couple, Tidswell and Doughty [31] suggested the formation of a radical on sulpholane as,

$$BF_4^- \xrightarrow{-e^-} BF_4^{-\bullet} \rightarrow BF_3 + F^\bullet$$
$$F^\bullet + HS \rightarrow HF + S^\bullet \qquad HS: \text{Sulpholane}$$

A similar reaction mechanism as shown below may also be expected for the reaction of acetonitrile, where the polymerization may propagate by the reaction of C=C double bond and by the oxidation of $-NH_2$ group.

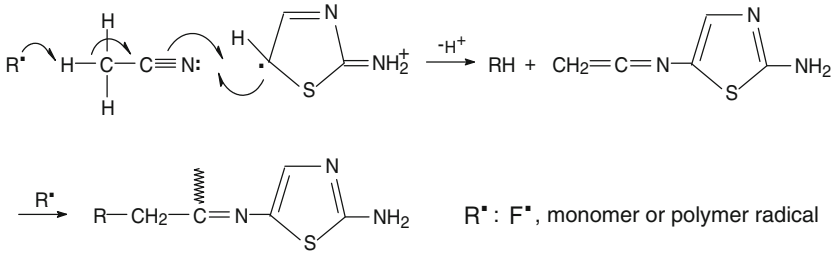

The electronic absorption spectra observed for the DMSO solutions of AT and PAT are shown in Fig. 9. The π–π^* transition of the thiazole ring was observed at 267 nm (Fig. 9a) and the broad absorption band at around 370 nm, with a long tail extending to 600–700 nm assigned to the π–π^* transition of the conjugated polymer (Fig. 9b) [16, 21].

The conductivity of PAT was measured to be about 10^{-6} S/cm by four-probe technique, whereas it increased up to about 10^{-3} S/cm upon doping of the polymer with I_2 at 55 °C under vacuum.

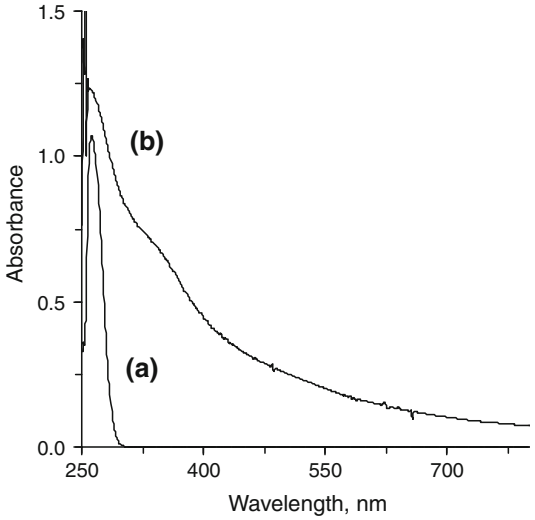

Fig. 9 Electronic absorption spectra of DMSO solutions of AT (*a*) and PAT (*b*)

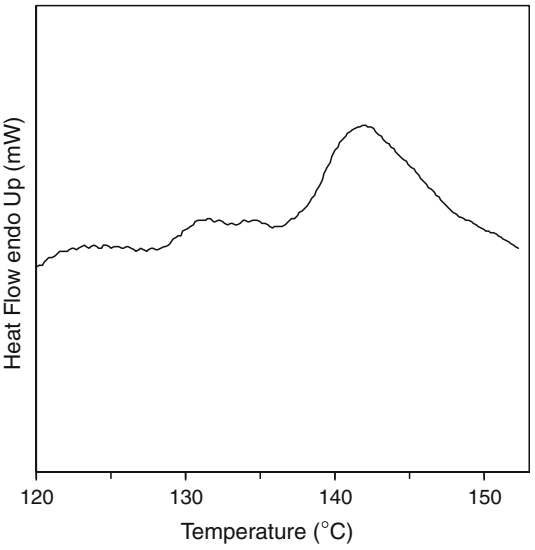

Fig. 10 DSC thermogram of PAT

DSC thermogram of PAT is shown in Fig. 10. The thermogram indicated two endothermic transitions at about 130 and 139 °C. The transition at 130 °C disappeared during the repetitive measurements carried out between 70 and 150 °C, while the transition at 139 °C was not affected. Therefore, the low temperature transition was decided to be due to the evaporation of low molecular weight volatiles and the transition at 139 °C attributed to the glass transition temperature, T_g, of the polymer.

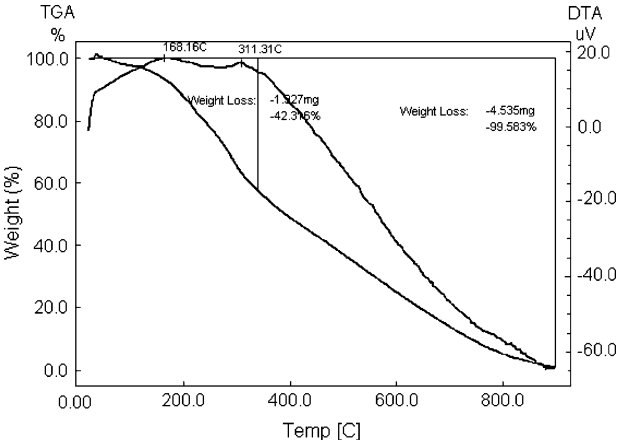

Fig. 11 TGA thermogram of PAT

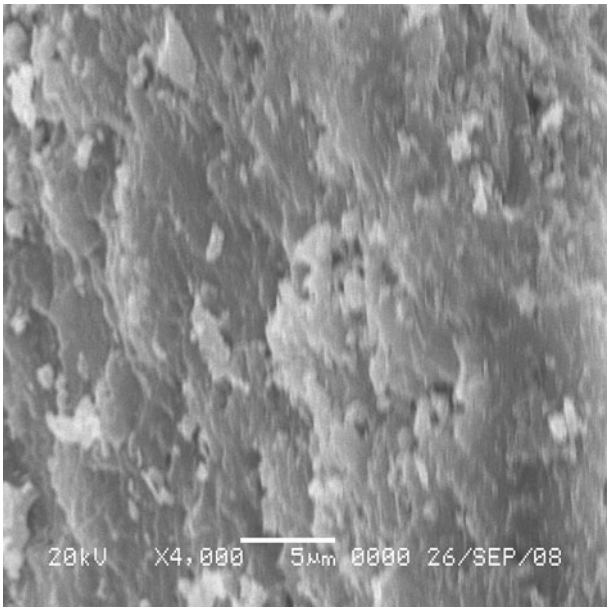

Fig. 12 SEM micrograph of PAT

TGA thermogram of PAT showed a typical three-step weight loss behavior (Fig. 11) [7, 32]. In the first step, 5% weight loss at temperatures up to 170 °C was observed. This is attributed to the evaporation of low molecular weight fragments present in the polymer. The second weight loss step occurred between 170–310 °C and the weight loss at 310 °C was about 42%. This can be attributed to the loss of dopant anions, BF_4^-, accompanied with the degradation of PAT chains. The third step started at 310 °C and complete weight loss observed at 900 °C.

The SEM micrograph of PAT is shown in Fig. 12. The micrograph indicates that PAT flakes are accumulated on each other with a non-porous, rough surface.

Conclusion

AT can be polymerized in acetonitrile-TBAFB, solvent-electrolyte couple by the electrochemical oxidation. A soluble conducting polymer with a molecular weight of 7320 g/mol was obtained. The polymer yield increased with increasing polymerization time and temperature and about 75% yield was achieved from the CPE carried out at 40 °C for 48 h. Conductivity of the polymer was measured to be about 10^{-6} S/cm, which increased up to 10^{-3} S/cm upon doping with iodine. Structural analyses indicated that AT polymerizes via oxidation of $-NH_2$ group and formation of –N(H)– linkages between the AT rings. It was also shown that acetonitrile may participate in the polymerization reactions and enter into the structure of the polymer.

Acknowledgment The authors are grateful to Kırıkkale University Research Fund, BAP-2006/13, for support of this work.

References

1. Odacı D, Kayaham SK, Timur S, Toppare L (2008) Use of thiophene-based conducting polymer in microbial biosensing. Electrochim Acta 53:4104–4108
2. Retama JR, Mecerreyes D, Lopez-Ruiz B, Lopez-Cabarcos E (2005) Synthesis and characterization of semiconducting polypyrrole/polyacrylamide microparticles with GOx for biosensor applications. Colloids Surf A 270:239–244
3. Armelin E, Pla R, Liesa F, Ramis X, Iribarren JI, Aleman C (2008) Protection with polyaniline and polypyrrole as anticorrosive additives for epoxy paint. Corros Sci 50:721–728
4. Bereket G, Hür E, Şahin Y (2005) Electrodeposition of polyaniline, poly(2-iodoaniline), and poly(aniline-co-2-iodoaniline) on steel surfaces and corrosion protection of steel. Appl Surf Sci 252:1233–1244
5. Sjöberg-Eerola P, Nylund J, Bobacka J, Lewenstam A, Ivaska A (2008) Soluble semiconducting poly(3-octylthiophene) as a solid-contact material in all-solid-state chloride sensor. Sensors Actuators B 134:878–886
6. Lindfors T, Ivaska A (2001) Calcium-selective electrode based on polyaniline functionalized with bis[4-(1,1,3,3-tetranethylbutyl)phneyl]phosphate. Anal Chim Acta 437:171–182
7. Bezgin B, Cihaner A, Önal A (2008) Electrochemical polymerization of 9-fluorenecarboxylic acid and its electrochromic device application. Thin Solid Films 516:7329–7334
8. Kobayashi T, Yoneyama H, Tamura H (1984) Polyaniline film-coated electrodes as electrochromic display devices. J Electroanal Chem 161:419–423

9. Walkowiak M, Schroeder G, Gierczyk B, Waszak D, Osinska M (2007) New lithium ion conducting polymer electrolytes based on polysiloxane grafted with Si-tripodand centers. Electrochem Commun 9:1558–1562
10. Rehan HH (2003) A new polymer/polymer rechargeable battery: polyaniline/$LiClO_4$(MeCN)/poly-1-naphthol. J Power Sources 113:57–61
11. Syed AA, Dinesan MK (1991) Review: polyaniline—a novel polymeric material. Talanta 38(8):815–837
12. Ahuja T, Mir IA, Kumar D, Rajesh D (2008) Potentiometric urea biosensor based on BSA embedded surface modified polypyrrole film. Sensors Actuators B 134:140–145
13. Ye S, Girard F, Belanger D (1993) Impedance study of polypyrrole films doped with tetrathiomolybdate anions and containing molybdenum trisulfide. J Phys Chem 97:12373–12378
14. Kabasakaloğlu M, Talu M, Yıldırım F, Sarı B (2003) The electrochemical homopolymerization of furan and thiophene and the structural elucidation of their bipolymer films. Appl Surf Sci 218:84–96
15. Dong S, Zhang W (1989) Study on conducting polythiophene electrochemically polymerized in phosphoric acid aqueous solution. Synth Met 30:359–369
16. İmamoğlu T, Önal AM (2007) Electrochemical polymerisation of 2-aminofluorene in ethylalcohol/water medium. Eur Polym J 40:1875–1880
17. Chandrasekhar P, Gumbs RW (1991) Electrosynthesis, spectroelectrochemical, electrochemical, and chronovoltabsorptometric properties of family of poly(aromatic amines), novel processible conducting polymers. J Electrochem Soc 138(5):1337–1346
18. Catellani M, Destri S, Porzio W (1988) Thiazole-based polymers: synthesis, characterization and electronic structure. Synth Met 26:259–265
19. Bolognesi A, Catellani M, Destri S, Porzio W (1987) Polythiazole: a new semiconducting polymer having a heteroatom in the conduction pathway. Synth Met 18:129–132
20. Maruyama T, Suganuma H, Yamamoto T (1995) Preparation of π-conjugated polythiazoles and their electrically conducting properties. Synth Met 74:183–185
21. Solmaz R, Kardaş G (2009) Electrochemical synthesis and characterization of poly-2-aminothiazole. Prog Org Coat 64:81–88
22. Sayyah SM, EL-Deeb SM, Abdel-Rehim SS (2004) Electropolymerization of 2-amino-4-phenylthiazole and characterization of the obtained polymer films. Int J Polym Mater 53:941–958
23. Sayyah SM, Kamal SM, Abd El-Rehim SS (2006) Electrochemical polymerization of 2-amino-4-(4-methoxyphenyl)thiazole and characterization of the obtained polymer. Int J Polym Mater 55:79–101
24. Nicholson RS, Shain I (1964) Theory of stationary electrode polarography: single scan and cyclic methods applied to reversible, irreversible, and kinetic systems. Anal Chem 36:706–723
25. Newitt EJ, Kokle V (1966) Molecular structure of polyethylene. XIII. An improved cryoscopic method for determining number average-molecular weight of polyethylene. J Polym Sci A 4:705–714
26. Fleischmann M, Pletcher D (1968) The electrochemical oxidation of some aliphatic hydrocarbons in acetonitrile. Tetrahedron Lett 60:6255–6258
27. Folley JK, Korzeniewski C, Pons S (1988) Anodic and cathodic reactions in acetonitrile/tetra-*n*-butylammonium tetrafluoroborate: an electrochemical and infrared spectrochemical study. Can J Chem 66:201–207
28. Akbulut U, Fernandez JE, Brike RL (1975) Electroinitiated cationic polymerization of styrene by direct electron transfer. J Polym Sci Polym Chem Ed 13:133–149
29. Testereci HN, Akın-Öktem G, Öktem Z (2004) Electrochemical polymerization of 4-allyl-1,2-dimethoxybenzene. React Funct Poym 61:183–189
30. Silverstein RM, Bassler GC, Morill TC (1991) Spectrometric identification of organic compounds, 5th edn. Wiley, New York
31. Tidswell BM, Doughty AG (1971) The electroinitiated polymerization of styrene: part 1. Polymer 12:431–443
32. Patil SF, Bedekar AG, Patil RC, Agashet C (1994) Optical and thermal characterization of poly(*o*-methylaniline) films. Indian J Chem 33A:580–582